ORIGINAL ARTICLE



Single-cell transcriptome provides novel insights into antler stem cells, a cell type capable of mammalian organ regeneration

Hengxing Ba 1 · Datao Wang 1 · Weiyao Wu 2 · Hongmei Sun 1 · Chunyi Li 1,3

Received: 28 October 2018 / Accepted: 9 January 2019

© Springer-Verlag GmbH Germany, part of Springer Nature 2019

Abstract

Antler regeneration, a stem cell–based epimorphic process, has a potential as a valuable model for regenerative medicine. A pool of antler stem cells (ASCs) for antler development is located in the antlerogenic periosteum (AP). However, whether this ASC pool is homogenous or heterogeneous has not been fully evaluated. In this study, we produced a comprehensive transcriptome dataset at the single-cell level for the ASCs based on the 10^{\times} Genomics platform (scRNA-seq). A total of 4565 ASCs were sequenced and classified into a large cell cluster, indicating that the ASC resident in the AP are likely to be a homogeneous population. The scRNA-seq data revealed that tumor-related genes were highly expressed in these homogeneous ASCs, i.e., TIMP1, TMSB10, LGALS1, FTH1, VIM, LOC110126017, and S100A4. Results of screening for stem cell markers suggest that the ASCs may be considered as a special type of stem cell between embryonic (CD9) and adult (CD29, CD90, NPM1, and VIM) stem cells. Our results provide the first comprehensive transcriptome analysis at the single-cell level for the ASCs and identified only one major cell type resident in the AP and some key stem cell genes, which may hold the key to why antlers, the unique mammalian organ, can fully regenerate once lost.

Keywords Antler · Stem cell · Antlerogenic periosteum · Single cell · Transcriptome · scRNA-seq

Introduction

The "Holy Grail" of modern regenerative medicine is to grow back lost organs or appendages, which is known as epimorphic regeneration (RJ 1983; Stocum 2006). Our current knowledge of epimorphic regeneration is largely gained from the studies on lower vertebrates (Gardiner et al. 2002). Notably, these animals have the ability to reprogram phenotypically committed cells at the amputation plane toward an

Hengxing Ba and Datao Wang contributed equally to this work

Electronic supplementary material The online version of this article (https://doi.org/10.1007/s10142-019-00659-2) contains supplementary material, which is available to authorized users.

Chunyi Li lichunyi1959@163.com

Published online: 23 January 2019

- State Key Laboratory for Molecular Biology of Special Wild Economic Animals, Institute of Special Wild Economic Animals and Plants, Chinese Academy of Agricultural Sciences, Changchun 130112, China
- BGI Genomics, BGI-Shenzhen, Shenzhen 518083, China
- Changchun Sci-Tech University, Changchun, China

embryonic-like cell phenotype (de-differentiation) and to form a cone-shaped tissue mass, known as a blastema (Mescher 1996). Deer antlers are the only mammalian appendages capable of full renewal and therefore offer a unique opportunity to explore how nature has solved the problem of epimorphic regeneration in mammals (Goss 1995; Kierdorf and Li 2009; Li et al. 2009; Li 2012). Recent studies concluded that antler regeneration is a stem cell–based epimorphic process (Kierdorf et al. 2007; Li et al. 2005, 2007a; Rolf et al. 2008) and has the potential for development as a valuable model for biomedical research and regenerative medicine. Revealing the mechanism underlying this stem cell–based epimorphic regeneration in mammals would undoubtedly place us in a better position to promote tissue/organ regeneration in humans.

Antlers regenerate from the permanent cranial bony protuberances, known as pedicles. Growth of a pedicle itself is initiated when a male deer approaches puberty. The origin is a piece of periosteum, known as antlerogenic periosteum (AP), which covers the frontal crest on the skull (Li 1994). Removal of the AP prior to pedicle initiation stops pedicle and antler growth, and transplantation of the AP autologously induces ectopic pedicle and antler formation (Goss and Powel



1985; Li et al. 2002; Li et al. 2007b). The initial discovery of the AP (Hartwig and Schrudde 1974) has been hailed as a "hallmark" event in antler research history (RJ 1983). The AP tissue, ~ 2.5 cm in diameter and 2.5–3 mm in thickness, contains around five million cells, which sustain the seasonal renewal of the entire antlers throughout the deer's life (Li et al. 2009). The potency of the AP cells has been investigated by several laboratories (Berg et al. 2007; Li and Suttie 2001; Price et al. 2005a; Rolf et al. 2008). The AP cells can be induced in vitro to differentiate into chondrocytes, osteoblasts, adipocytes, myoblasts, and neural-like cells. Therefore, AP cells have been termed antler stem cells (ASCs) and are essential for full regeneration of this unique mammalian organ (Li et al. 2009).

Differences in cell type within any tissue are essential for their biological states and function. Numerous studies in cell biology have utilized single-cell sequencing by employing new protocols of single-cell isolation to characterize functionally heterogeneous cells (Yu and Lin 2016). This study is the first to apply single-cell sequencing technology to investigate the ASCs through transcriptome (scRNA-seq) using the 10× Genomics platform, a droplet-based system that enables 3′ messenger RNA (mRNA) digital counting for thousands of single cells (Zheng et al. 2017).

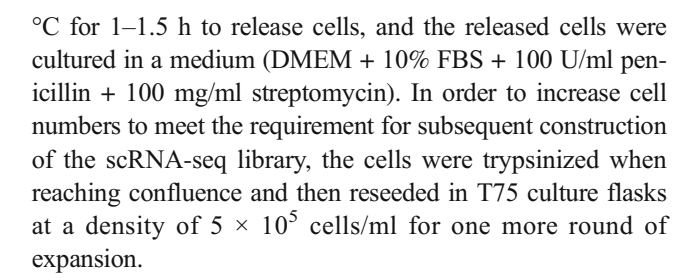
Materials and methods

AP tissue sampling

The AP tissues were obtained from a 6-month-old male sika deer immediately after slaughtering, according to the previous protocol (Li and Suttie 2003). Briefly, to collect the AP tissue, a crescent-shaped incision was made on the scalp skin 2 cm medial to the frontal crest; the skin was separated from the frontal bone to expose the AP. The AP was then peeled from the underlying bone following the delineating incisions cut on the periosteum and then placed into 50 ml of centrifuge tube containing 20 ml cold DMEM (Gibco; Grand Island, USA) plus 500 U/ml penicillin and 500 g/ml streptomycin (Invitrogen, USA). All experimental processes were approved by the Animal Ethics Committee of Institute of Special Wild Economic Animals and Plants, Chinese Academy of Agricultural Sciences (CAAS2017015).

Isolation of the AP cells

Isolation of the AP cells was carried out according to our previous methodology (Li et al. 1999, 2012). Briefly, after sampling, AP tissue was immediately cut into thin slices (around 0.7 mm in thickness) using a custom-built tissue cutter (Chu et al. 2017). These slices were digested in the DMEM culture medium containing collagenase (150 units/ml) at 37



Single-cell sequencing using Chromium™ platform

The scRNA-seq library was constructed using the Chromium™ Controller and Chromium™ Single-Cell 3' Reagent Version 1 Kit (10× Genomics, Pleasanton, CA) to generate single-cell gel bead-in-emulsions (GEMs) as previously described (Zheng et al. 2017). Briefly, about 5 \times 10⁵/ml (500/µl) suspended cells were obtained and placed on the ice. In total, a 15-µl cellular suspension that contained ~ 7500 cells was added to the Master Mix in the tube strip well. The 100-µl Master Mix-containing cells, 40 μl single-cell 3' gel beads, and 135 μl oil surfactant solution were transferred to each well in the ChromiumTM single-cell 3' chip row. Subsequently, GEM-RT was performed using Thermocycler (BioRad; 55 °C for 2 h, 85 °C for 5 min, held at 4 °C). Post GEM-RT cleanup and cDNA amplification was performed to isolate and amplify cDNA for library construction. The samples were sequenced in two lanes on the HiSeg 2500 in rapid run mode using a paired end flow cell: Read1 98 cycles, Index1 14 cycles, Index2 8 cycles, and Read2 10 cycles.

scRNA-seq data analysis

Cell Ranger Software Suite version 1.3.1 (http://support. 10xgenomics.com/) was used to perform sample demultiplexing, barcode processing, and single-cell 3' gene counting, as performed previously (Zheng et al. 2017). The 10-bp transcripts/unique molecular identifier (UMI) tags were extracted from Read2. Cellranger mkfastq used bcl2fastq v2.19 (https://support.illumina.com/) to demultiplex raw base call files from Hiseq2500 sequencer into sample-specific FASTQ files. Cellranger mkref was run to produce a cellranger-compatible reference based on both the Ovir.te1.0 genome sequences and the transcriptome GTF file. These FASTQ files were aligned to the reference with cellranger count that used an aligner called STAR (Dobin et al. 2013).

The cells were selected based on the following criteria (Yan et al. 2017): (1) the number of expressed genes (300–5000); (2) the number of UMI counts (< 25,000); (3) the percentage of mitochondrial genes (< 5%); and (4) the number of cells expressed per gene (≥ 5). After normalizing expressed data by NormalizeData function, dispersion of each gene against the



mean expression level was plotted using FindVariableGenes function (x.low.cutoff = 0.01, x.high.cutoff = 4, y.cutoff = 0.3), which was in Seurat R package version 2.2.1 (Butler et al. 2018). A total of 2943 variable genes were selected based on their plotting results (Fig. S1) and the amount of variability was found to be explained by cell cycle genes. The cell cycle scores were further generated by CellCycleScoring function based on G2/M and S phase markers, and then, these cores were used to scale cell-gene expression data using ScaleData function. The standard deviations of the principle components were plotted by PCElbowPlot function to identify the true dimensionality of a dataset (Fig. S2). Based on unsupervised graph-based nearest neighbor clustering algorithm with different resolution degrees, the scaled expression datasets were clustered using FindClusters function with the first 30 principal components according to the principal components analysis elbow plot. The cluster results were presented using t-distributed stochastic neighbor embedding (t-SNE)-based plots (Blondel et al. 2008). The FindAllMarkers function was used to find differentially expressed genes with absolute log2 fold change > 1 and adjust P value < 0.001.

Immunofluorescent staining

The primary cultured ASCs were fixed with 4% paraformal-dehyde for 30 min and blocked by incubation in 3% BSA (0.1% Triton X-100 for NPM1) in PBS for 1 h at RT, followed by incubation with the primary antibodies overnight at 4 °C. The cells were incubated with secondary antibody for 30 min followed by DAPI (blue) staining for visualization of nuclei. The primary and secondary antibodies used in the study are listed in Table S1. The primary antibodies were replaced by rabbit or mouse IgG for the isotype-matched controls. All images were captured under a fluorescent microscope (EVOS, ThermoFisher, USA).

Flow cytometry analysis

The ASCs were incubated with the primary antibodies overnight at 4 °C, and then the cells were stained with FITC-conjugated secondary antibodies for another 1 h at RT. Isotype-matched rabbit or mouse IgG was used as a negative control. After three times of washes with cold PBS, the cells were resuspended in 500 µl PBS. Flow cytometry analysis was performed using FACSCalibur and the results were analyzed using Cellquest software (BD Biosciences, USA).

Data availability The raw single-cell RNA-seq data in fastq format can be found at SRA under BioProject PRJNA416396.

Results

High-quality scRNA-seq data

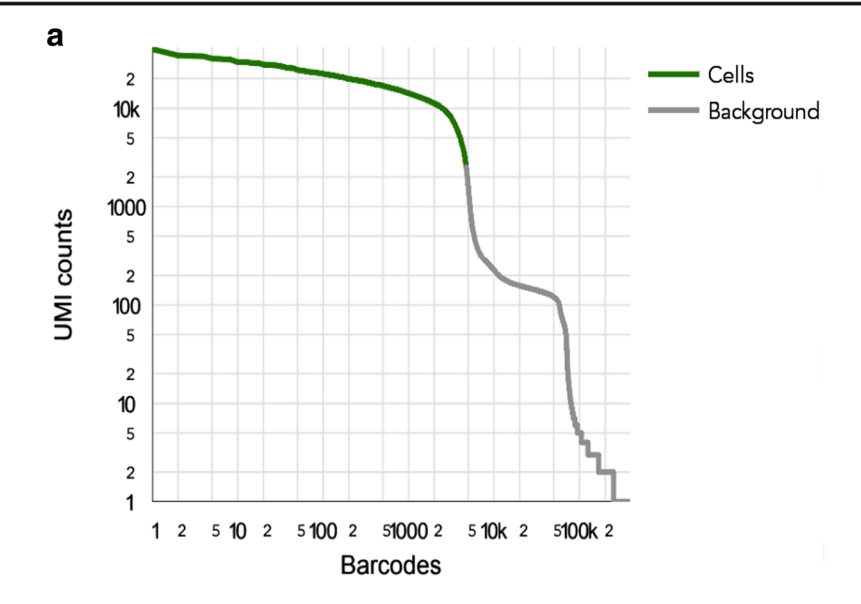
A total of 252,818,309 read pairs were mapped to 14,993 genes, which were found to be expressed in the 4731 sorted individual ASCs. This was equivalent to an average of 53,438 mapped read pairs per cell, which is reportedly sufficient for an accurate analysis by single-cell 3' solution (Yan et al. 2017). The median gene number and UMI counts were 2568 and 10,309 respectively. The results of detailed statistical analysis of the scRNA-seq data and the sequenced cells are summarized in Table S2 and S3 respectively.

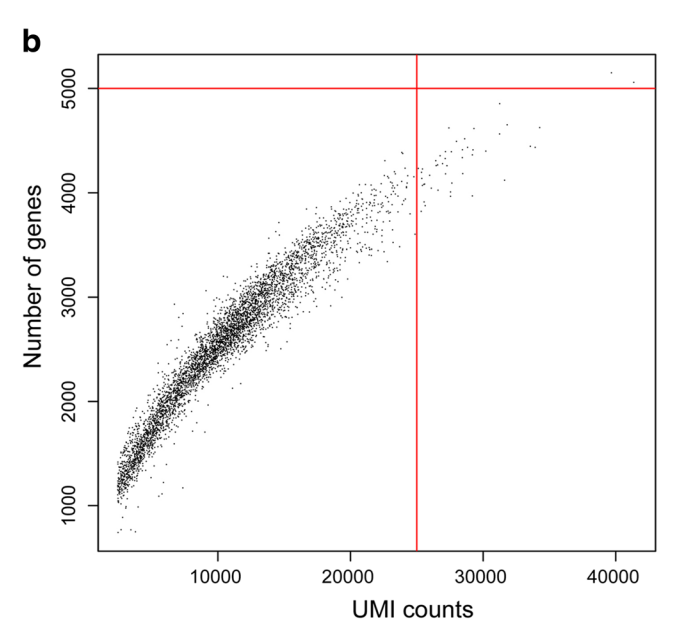
A steep drop-off of barcode UMI counts was indicative of good separation of the cell-associated barcodes from the empty droplets (Fig. 1a). The number of genes (Fig. 1b) and percentage of mitochondrial genes (Fig. 1c) against the corresponding UMI counts per cell were plotted respectively to exclude outlier cells as potential multi-cell droplets. Based on the threshold criteria (see Methods), we filtered out 116 cells and 1820 genes. Altogether, 4615 singular cells and 13,173 genes were retained for further analysis.

A large cell cluster across the ASCs

The graph-based nearest neighbor clustering algorithm that did not rely on known markers uncovered two cell clusters from 4615 high-quality cells with a resolution degree of 0.1 (Fig. 2a). We further defined groups of genes (absolute log2 fold change > 1 and adjust P value < 0.001), which allowed classification of these cells into two distinct cell clusters (Fig. 2b). We found no upregulated genes in the small cluster (50 cells). However, a high proportion of downregulated mitochondrial genes (i.e., MT-COX1, MT-COX2, MT-COX3, MT-ND2, MT-ND1, and MT-CYTB) were represented, strongly suggesting that the small cluster could be contaminated by debris of the ASCs. We also found the ASCs in the large cell cluster (4565 cells) expressed high levels of extracellular matrix proteins, such as collagen family. In particular, these genes (i.e., COL1A1, COL1A2, COL5A1, COL5A2, SPARC, and FN1) were typically applied to measure differentiated states from mesenchymal stem cell to osteoblast, osteoprogenitor, and chondrogenesis. Based on the resolution degree of 0.2, the large cell cluster was again separated into two clusters with 2404 and 2161 cells respectively (Fig. 2c), but only four genes had values of absolute log2 fold change > 1 and < 2 (ACTA2, THBS1, TNC, and MYL9) (Fig. 2d), indicating that the ASC residents in the AP are likely to represent a homogeneous population.







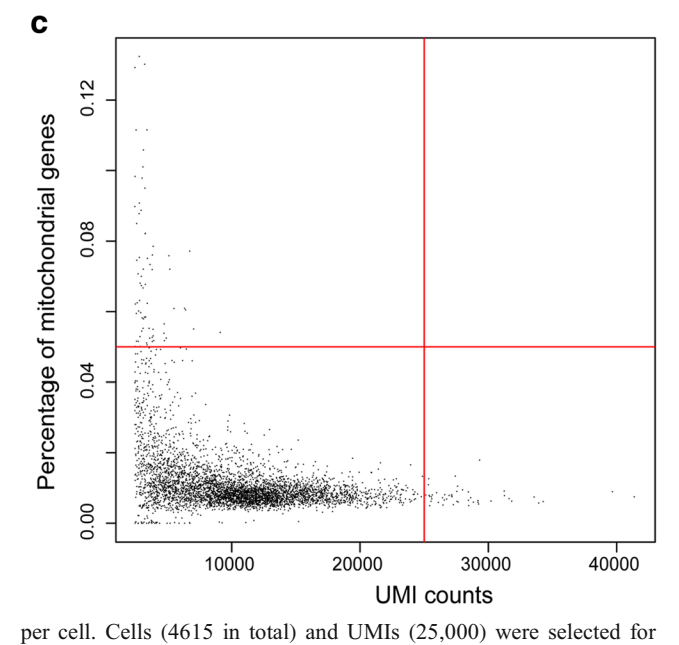


Fig. 1 Quality metrics of the ASC single-cell transcriptomes using 10^{\times} Genomics. **a** Barcode rank plot. In the plot, a steep drop-off is indicative of good separation between the cell-associated barcodes and the barcodes associated with empty partitions. **b** Plot between the numbers of genes and UMI counts per cell. **c** Plot of mitochondria UMIs and UMI counts

downstream analysis (red dashed lines). Cells with number of genes < 5000 and > 300, UMI counts < 25,000, and the percentage of mitochondrial genes < 5% were selected for downstream analysis (red dashed lines)

Highly expressed genes across the ASCs

A total of 35 genes were found to be highly and commonly expressed in cells of the large cell cluster (at least 20 UMIs); these were further sorted based on their expression levels (Fig. 3a and Table S4). Of the selected 35 genes, the first seven, i.e., metalloproteinase inhibitor 1 (TIMP1), thymosin beta 10 (TMSB10), galectin-1 (LGALS1), ferritinheavy chain (FTH1), vimentin (VIM), ferritin light chain-like genes (LOC110126017), and S100A4, were found to be expressed

over 50 UMIs. Almost all of the ASCs expressed these genes above the level of 10 UMIs. Notably, 98% and 90% of the ASCs expressed TMSB10 gene above the level of 30 and 50 UMIs respectively. The expression levels of the TMSB10, LGALS1 (Fig. 3b), and VIM genes (refer to Fig. 4a) were further confirmed using immunofluorescent staining. Of the selected 35 genes, 25 (71%) were found to be involved in the protein-protein interaction network in the STRING v10.5 (Fig. 3c), suggesting that they may come together to accomplish a particular biological function within the ASCs.



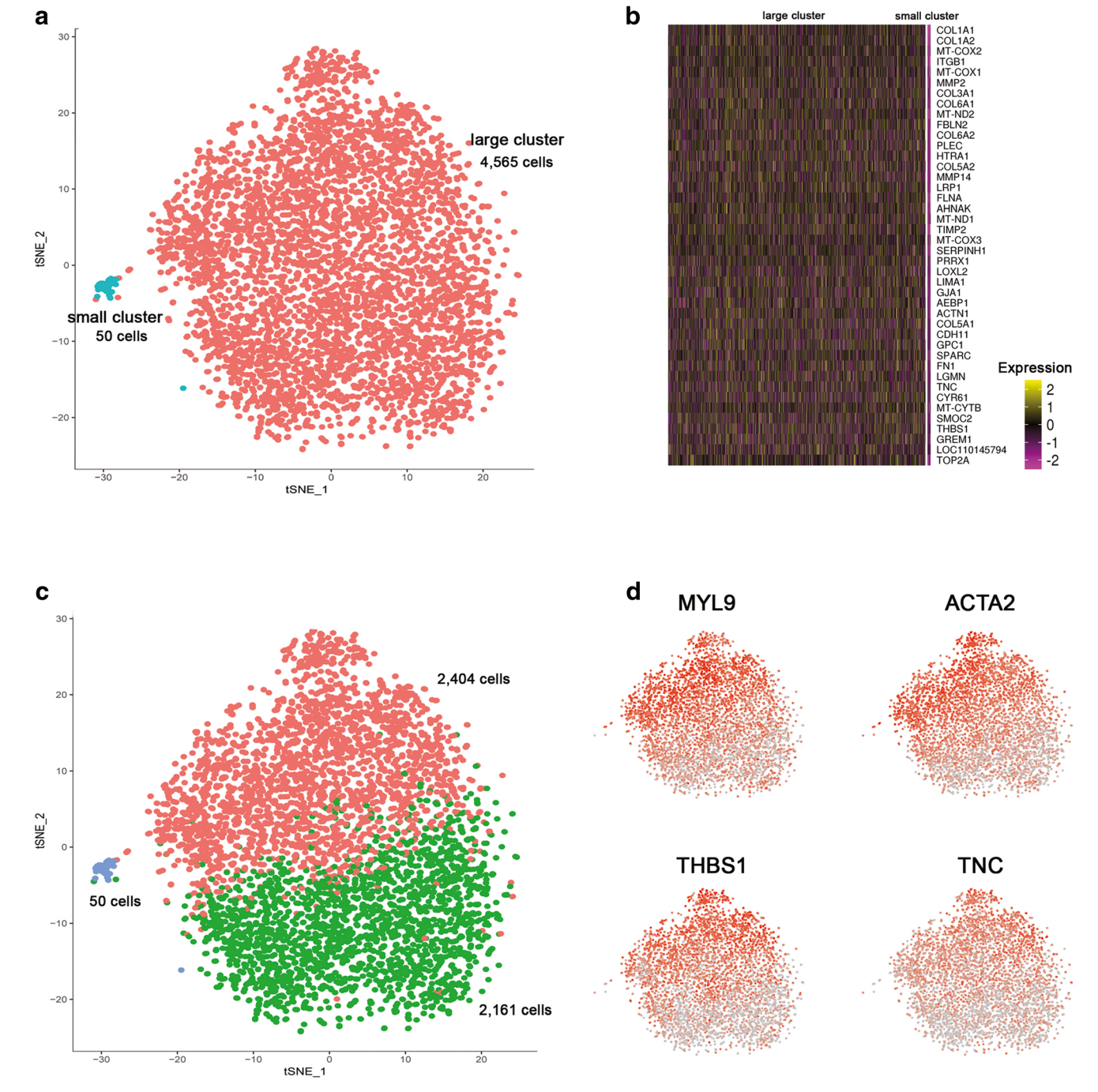


Fig. 2 Unsupervised graph-based nearest neighbor clustering analysis of the ASCs. **a** t-SNE projection of single cells, colored by two inferred ASC clusters based on the resolution degree of 0.1. **b** A normalized expression (centered) of differentially expressed genes (rows) from each of two clusters (columns) is shown in a heat map. Gene symbols are

represented at the right. **c** t-SNE projection of single cells, colored by three inferred ASC clusters based on the resolution degree of 0.2. **d** Four genes that have values of absolute log2 fold change > 1 and < 2 are labeled on t-SNE plots

Expression of stem cell markers

In order to investigate expression status of stem cell markers for the ASCs in the large cell cluster, we selected 16 marker genes from the scRNA-seq data based on two criteria: (1) expressed in at least one UMI count and (2)

expressed in over 3% of the ASCs. These 16 marker genes were then classified into four types of stem cell markers based on the definition for each type from the literature: (1) mesenchymal stem cell markers (10; CD29, CD73, CD105, CD90, fibronectin (FN1), VIM, nucleophosmin (NPM1), PDGFRA, CD44, and CD49);



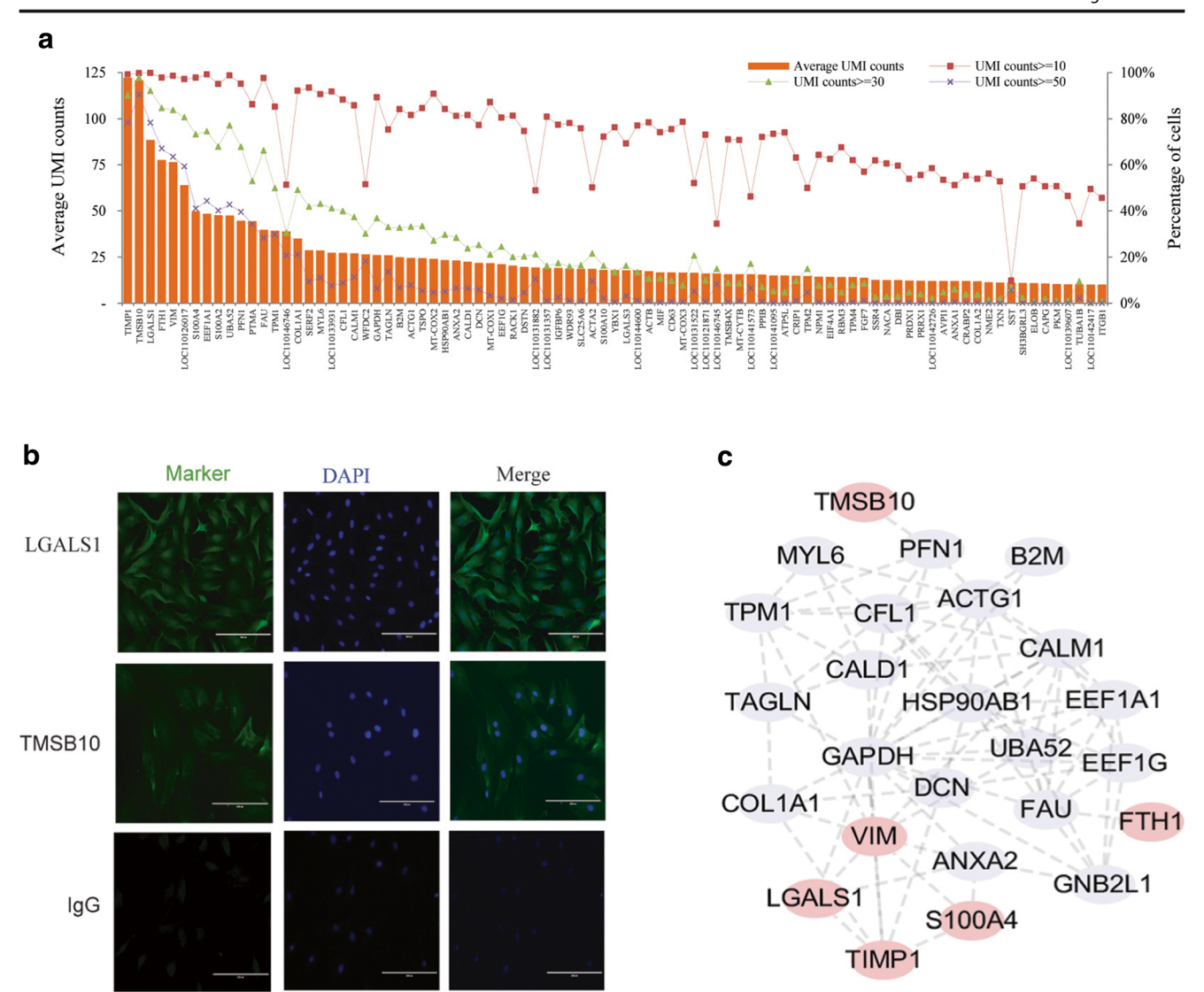


Fig. 3 Highly expressed genes in the scRNA-seq data. a Top 35 genes that were expressed at \geq 20 UMI averaged across all the ASCs (bar plot). Percentage of cells based on \geq 10, 30, and 50 UMIs per cell respectively (line plot). b Immunostaining of the ASCs using anti-TMSB10 and anti-

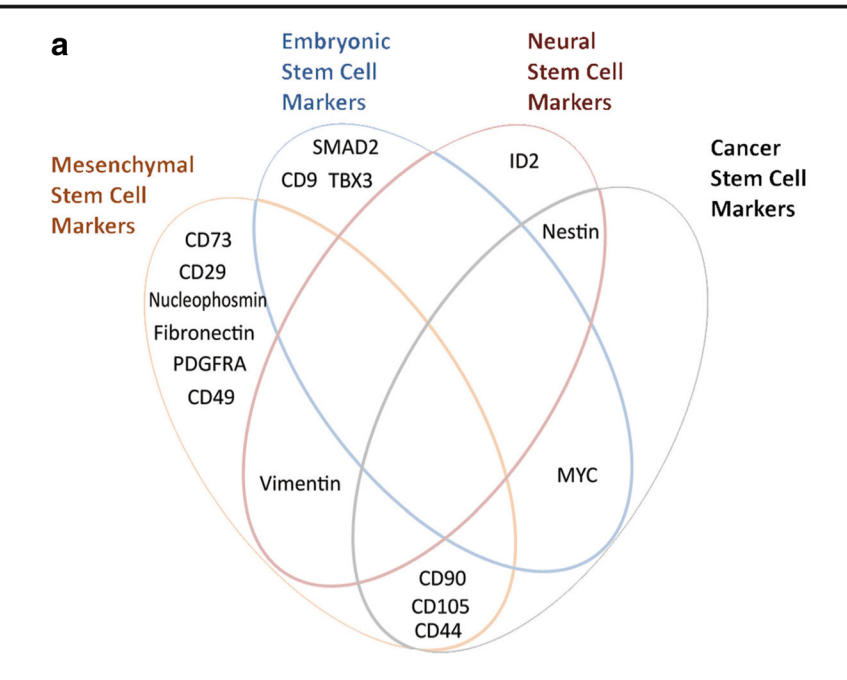
LGALS1. DAPI staining was used for nuclei detection. IgG staining was used as negative control. Scale bar: $200 \mu m$. c Protein-protein interaction network between 25 of the top 35 genes based on STRING v10.5 (string-db.org) searching with medium confidence (0.4)

(2) embryonic stem cell markers (4; CD9, SMAD2, MYC, and TBX3); (3) neural stem cell markers (3; ID2, nestin (NES), and VIM); and (4) cancer stem cell markers (4; CD44, MYC, CD90, and CD105) (Fig. 4a). When the expression level was set at nUMI > 5, four mesenchymal (CD90, CD29, VIM, and NPM1) and one embryonic stem cell marker genes (CD9) were found to be expressed in over 40% of the ASCs (Fig. 4b). More significantly, VIM, known as a neural stem cell marker (Bramanti et al. 2010), was highly expressed in almost all of the ASCs.

High expression levels for these five stem cell marker genes (CD9, CD90, CD29, VIM, and NPM1) were further confirmed using immunofluorescent staining (Fig. 5a). In addition, the immunofluorescent staining results provided extra information over the expression level

study. For example, one of the NPM1 functions is to act on genomic stability and DNA repair (Lindstrom 2011), and in our results, distinct dots were clearly evident within and around the nucleus of the ASCs, suggesting that it is a nucleus protein. Also as expected, VIM, a major cytoskeletal protein of mesenchymal cells (Colucci-Guyon et al. 1994; Goldman et al. 1996), was observed to be in a distinct form outside of nuclei. To further investigate the proportion of positive cells for each of these five marker genes, FACS analysis was performed and the results showed that CD9⁺, CD90⁺, CD29⁺, VIM⁺, and NPM1⁺ were positive in 91.1%, 93.2%, 92.8%, 98.4%, and 94.5% of ASCs respectively (Fig. 5b), which were concordant with the results of scRNA-seq data analysis.





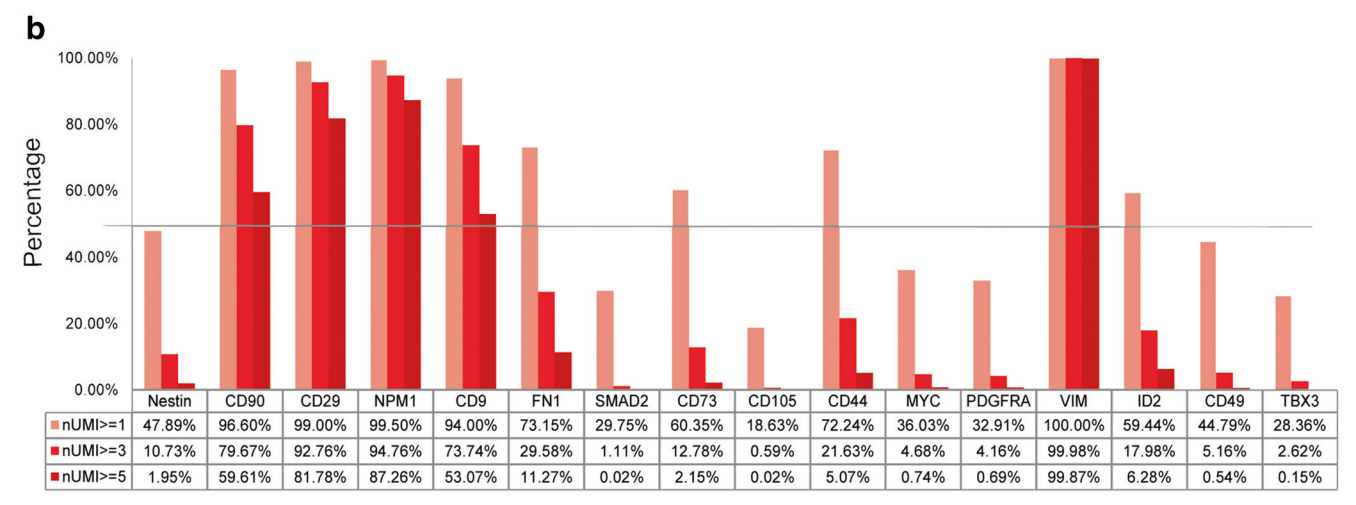


Fig. 4 ASC screening results using the currently available stem cell markers. These cells were labeled by 16 stem cell markers respectively, and the label threshold was set to meet a criterion that a marker must be expressed by more than 3% ASCs and with at least one UMI count. **a** Venn diagram of the 16 individual stem cell markers across the four types

of stem cell marker, including 10 mesenchymal stem cell markers, four embryonic stem cell markers, three neural stem cell markers, and five cancer stem cell markers. **b** Expression abundance of the 16 individual stem cell markers based on UMI counts \geq 1, 3, and 5

Discussion

Single-cell RNA sequencing (scRNA-seq) approaches have become increasingly popular providing insights into various aspects of developmental and stem cell biology (Kumar et al. 2017). In the present study, using the scRNA-seq technology based on the 10× Genomics platform, we provided an initial high-resolution picture of molecular characterization for the ASCs (4615 cells including 13,173 genes).

Several highly expressed genes, such as S100A4, LGALS1, and TMSB10, have been reported previously as being related to the development of the AP tissues/cells (Li et al. 2012; Park et al. 2004; Wang et al. 2017), and TMSB10

is also highly expressed in growing antlers (Lord et al. 2004; Zhang et al. 2018). These highly expressed genes are reportedly tumor-related factors. S100A4 promotes cell proliferation and tumor growth (Sherbet 2009). The downregulation of S100A4 expression suppresses cell proliferation in many cancer cells (Huang et al. 2012; Ma et al. 2010). LGALS1 modulates the immune response (Liu 2005; Rabinovich et al. 2007) and may contribute to immune privilege in tumors. TMSB10 plays important roles in the progression and metastasis of various tumors (Santelli et al. 1999; Sribenja et al. 2009; Zhang et al. 2017). The dysregulated activity of TIMP1 has been implicated in tumors (Kim et al. 2012). Methylation of VIM has been established as a biomarker of



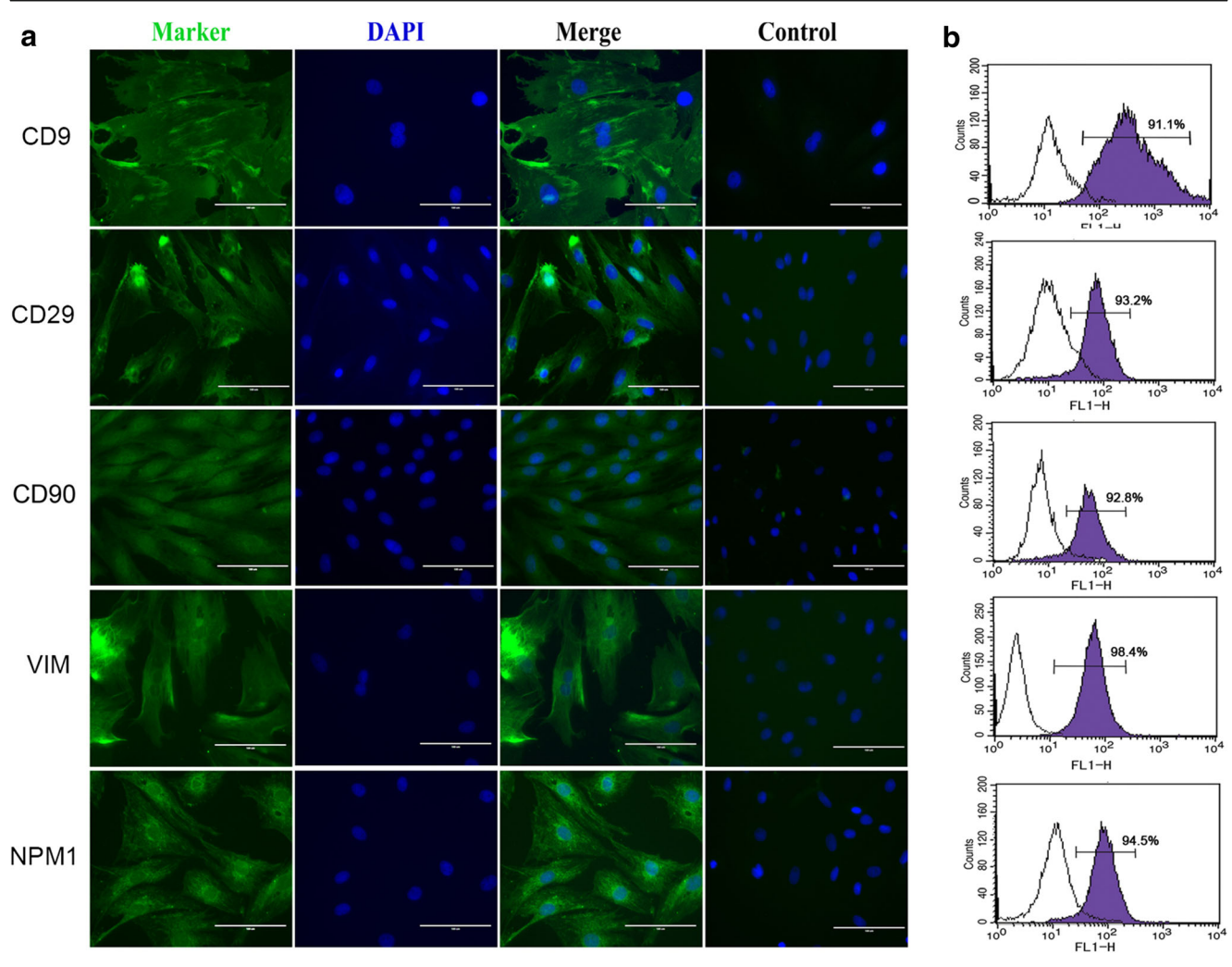


Fig. 5 Immunostaining and FACS analysis of the ASCs. **a** Immunostaining of ASCs using anti-CD9, anti-CD29, anti-CD90, anti-VIM, and anti-NPM1 antibodies. DAPI staining was used for detection of

nuclei. Scale bar: 200 μm . **b** FACS analysis was performed using each of these five antibodies. Values show the intensity of the indicated antigen

tumors (Jung et al. 2011). Both FTH1 and LOC110126017 (ferritin light chain-like) encode proteins that play important roles in iron storage and homeostasis. It is known that iron has a role in the tumor microenvironment and in metastasis and can contribute to both tumor initiation and tumor growth (Torti and Torti 2013). Although these tumor-related genes are highly expressed in the ASCs, these cells do not become cancerous during antler formation despite an astonishing rate of proliferation and differentiation, which is genuinely impressive and worth further exploration.

Recently, it has been reported that the ASCs express both mesenchymal stem cell markers, such as STRO-1 and CD105, and embryonic stem cell markers such as CD9 and MYC (Li et al. 2009; Rolf et al. 2008; Seo et al. 2014). Surprisingly, the ASCs were also reported to express some key embryonic stem cell marker genes, such as Oct4, SOX2, and NANOG (Li et al. 2009; Seo et al. 2014). However, we failed to detect the expression of these key embryonic marker genes through the scRNA-seq in this study. Interestingly, expressed NANOG

in the ASCs was found as a pseudogene in one of our previous studies (Wang et al. 2016). In addition, the ASCs have to be considered to be of neural crest origin (Kierdorf et al. 2007; Li and Suttie 2001; Price et al. 2005b), with a direct evidence being the detection of the mRNAs for several neural crest cell markers in the ASCs using RT-PCR (Mount et al. 2006). The neural crest cell population is an embryonic cell population and these cells might represent some kind of "embryonic remnant" comprising pluripotent cells left over from the early embryo (Li et al. 2009). Our results also showed that almost all of the ASCs highly expressed the VIM gene, a marker that appears at the earliest stage of neural tube development (Houle and Fedoroff 1983), which further supports the neural crest origin of the AP cells. Overall, despite the lack of expression of key embryonic marker genes in this study, the ASC may still be considered as a unique type of stem cell that has biological attributes derived from embryonic (CD9), mesenchymal (CD29, CD90, NPM1, and VIM), and neural stem cells (VIM). Our findings in this study strongly support the



view that the annual antler regeneration represents a stem cell-based process.

The scRNA-seq studies have thus far led to the discovery of novel cell types and provided insights into regulatory networks during development (Liu and Trapnell 2016). Using this powerful approach, we have successfully identified only one major type of ASC resident in the AP. It is understandable that, for such a small piece of tissue (around 2.5 cm in diameter and 2 mm in thickness) to initiate a large mammalian appendage (up to 15 kg) within 2 to 3 months of time, this limited number of cells (around five million) must uniformly possess stem cell attributes, such as almost unlimited proliferation potential. Whatever it is, the results from the present study provide a useful source for further investigation at molecular level of deer antler renewal, the only stem cell–based mammalian organ regeneration.

Acknowledgements We wish to thank Drs. Peter Fennessy and Eric Lord for reading through the paper and giving valuable comments.

Author contributions H.B., D.W., and C.L. conceived the experiment. D.W. collected the samples and performed molecular- and cell-related experiments. H.S. cultured the cell lines. W.W. extracted the RNA samples and prepared them for single-cell 3' library construction and sequencing. H.B. performed QC and data analysis. H.B., W.W., and C.L. wrote the manuscript. All authors read and approved the final manuscript.

Funding information This work was funded by the Strategic Priority Research Program of the Chinese Academy of Sciences (XDA16010403), Natural Science Foundation of Jilin Province (No. 20170101003JC) and Central Public-Interest Scientific Institution Basal Research Fund (No. 1610342019026).

Compliance with ethical standards

Competing interests The authors declare that they have no competing interests.

Publisher's note Springer Nature remains neutral with regard to jurisdictional claims in published maps and institutional affiliations.

References

- Berg DK, Li C, Asher G, Wells DN, Oback B (2007) Red deer cloned from antler stem cells and their differentiated progeny. Biol Reprod 77:384–394. https://doi.org/10.1065/biolrepod.106.058172
- Blondel VD, Guillaume JL, Lambiotte R, Lefebvre E (2008) Fast unfolding of communities in largenetworks. Journal of Statistical Mechanics. 2008:155–168https://doi.org/10.1088/1742-5468/2008/10/P10008
- Bramanti V, Tomassoni D, Avitabile M, Amenta F, Avola R (2010) Biomarkers of glial cell proliferation and differentiation in culture. Front Biosci (Schol Ed) 2:558–570
- Butler A, Hoffman P, Smibert P, Papalexi E, Satija R (2018) Integrating single-cell transcriptomic data across different conditions, technologies, and species. Nat Biotechnol 36:411–420. https://doi.org/10. 1038/nbt.4096

- Chu W, Zhao H, Li J, Li C (2017) Custom-built tools for the study of deer antler biology. Front Biosci (Landmark edition) 22:1622–1633
- Colucci-Guyon E, Portier MM, Dunia I, Paulin D, Pournin S, Babinet C (1994) Mice lacking vimentin develop and reproduce without an obvious phenotype. Cell 79:679–694
- Dobin A, Davis CA, Schlesinger F, Drenkow J, Zaleski C, Jha S, Batut P, Chaisson M, Gingeras TR (2013) STAR: ultrafast universal RNA-seq aligner. Bioinformatics 29:15–21. https://doi.org/10.1093/bioinformatics/bts635
- Gardiner DM, Endo T, Bryant SV (2002) The molecular basis of amphibian limb regeneration: integrating the old with the new. Semin Cell Dev Biol 13:345–352
- Goldman RD, Khuon S, Chou YH, Opal P, Steinert PM (1996) The function of intermediate filaments in cell shape and cytoskeletal integrity. J Cell Biol 134:971–983
- Goss RJ (1995) Future directions in antler research. Anat Rec 241:291–302. https://doi.org/10.1002/ar.1092410302
- Goss RJ, Powel RS (1985) Induction of deer antlers by transplanted periosteum. I Graft size and shape. J Exp Zool 235:359–373. https://doi.org/10.1002/jez.1402350307
- Hartwig H, Schrudde J (1974) Experimentelle Untersuchungen zur Bildung der primaren Stirnauswuchse beim Reh (Capreolus capreolus L.). Z Jagdwiss 20:1–13
- Houle J, Fedoroff S (1983) Temporal relationship between the appearance of vimentin and neural tube development. Brain Res 285:189–195
- Huang LY, Xu Y, Cai GX, Guan ZQ, Cai SJ (2012) Downregulation of S100A4 expression by RNA interference suppresses cell growth and invasion in human colorectal cancer cells. Oncol Rep 27:917–922. https://doi.org/10.3892/or.2011.1598
- Jung S, Yi L, Kim J, Jeong D, Oh T, Kim CH, Kim CJ, Shin J, An S, Lee MS (2011) The role of vimentin as a methylation biomarker for early diagnosis of cervical cancer. Mol Cell 31:405–411. https://doi.org/ 10.1007/s10059-011-0229-x
- Kierdorf U, Kierdorf H, Szuwart T (2007) Deer antler regeneration: cells, concepts, and controversies. J Morphol 268:726–738. https://doi. org/10.1002/jmor.10546
- Kierdorf U, Li CY, Price JS (2009) Improbable appendages: deer antler renewal as a unique case of mammalian regeneration. Semin Cell Dev Biol 20:535–542. https://doi.org/10.1016/j.semcdb.2008.11. 011
- Kim YS, Kim SH, Kang JG, Ko JH (2012) Expression level and glycan dynamics determine the net effects of TIMP-1 on cancer progression. BMB Rep 45:623–628. https://doi.org/10.5483/BMBRep. 2012.45.11.233
- Kumar P, Tan YQ, Cahan P (2017) Understanding development and stem cells using single cell-based analyses of gene expression. Development 144:17–32. https://doi.org/10.1242/dev.133058
- Li CY (2012) Deer antler regeneration: a stem cell-based epimorphic Process. Birth Defects Res C 96:51–62. https://doi.org/10.1002/ bdrc.21000
- Li C, Suttie JM (1994) Light microscopic studies of pedicle and early first antler development in red deer (Cervus elaphus). Anat Rec 239: 198–215. https://doi.org/10.1002/ar.1092390211
- Li C, Suttie JM (2001) Deer antlerogenic periosteum: a piece of postnatally retained embryonic tissue? Anat Embryol (Berl) 204:375–388
- Li C, Suttie JM (2003) Tissue collection methods for antler research. Eur J Morphol 41:23–30. https://doi.org/10.1076/ejom.41.1.23.28106
- Li C, Littlejohn RP, Suttie JM (1999) Effects of insulin-like growth factor 1 and testosterone on the proliferation of antlerogenic cells in vitro. J Exp Zool 284:82–90
- Li CY, Clark DE, Lord EA, Stanton JAL, Suttie JM (2002) Sampling technique to discriminate the different tissue layers of growing antler tips for gene discovery. Anat Rec 268:125–130. https://doi.org/10. 1002/ar.10120
- Li C, Suttie JM, Clark DE (2005) Histological examination of antler regeneration in red deer (Cervus elaphus). Anat Rec A Discov



- Mol Cell Evol Biol 282:163–174. https://doi.org/10.1002/ar.a. 20148
- Li C, Yang F, Li G, Gao X, Xing X, Wei H, Deng X, Clark DE (2007a) Antler regeneration: a dependent process of stem tissue primed via interaction with its enveloping skin. J Exp Zool A Ecol Genet Physiol 307:95–105. https://doi.org/10.1002/jez.a.352
- Li CY, Mackintosh CG, Martin SK, Clark DE (2007b) Identification of key tissue type for antler regeneration through pedicle periosteum deletion. Cell Tissue Res 328:65–75. https://doi.org/10.1007/ s00441-006-0333-y
- Li C, Yang F, Sheppard A (2009) Adult stem cells and mammalian epimorphic regeneration-insights from studying annual renewal of deer antlers. Curr Stem Cell Res Ther 4:237–251
- Li C, Harper A, Puddick J, Wang W, McMahon C (2012) Proteomes and signalling pathways of antler stem cells. PLoS One 7:e30026. https://doi.org/10.1371/journal.pone.0030026
- Lindstrom MS (2011) NPM1/B23: a multifunctional chaperone in ribosome biogenesis and chromatin remodeling. Biochem Res Int 2011: 195–209. https://doi.org/10.1155/2011/195209
- Liu FT (2005) Regulatory roles of galectins in the immune response. Int Arch Allergy Immunol 136:385–400. https://doi.org/10.1159/ 000084545
- Liu S, Trapnell C (2016) Single-cell transcriptome sequencing: recent advances and remainingchallenges. F1000research 5 https://doi. org/10.12688/f1000research.7223.1
- Lord EA, Clark DE, Martin SK, Pedersen GM, Gray JP, Li CY (2004) Profiling genes expressed in the regenerating tip of red deer (cervua elaphus) antler. Paper presented at the In advances in antler science and product technology
- Ma X, Yang YX, Wang YF, An GF, Lv G (2010) Small interfering RNA-directed knockdown of S100A4 decreases proliferation and invasiveness of osteosarcoma cells. Cancer Lett 299:171–181. https://doi.org/10.1016/j.canlet.2010.08.016
- Mescher AL (1996) The cellular basis of limb regeneration in urodeles. Int J Dev Biol 40:785–795
- Mount JG, Muzylak M, Allen S, Althnaian T, Mcgonnell IM, Price JS (2006) Evidence that thecanonical Wnt signalling pathway regulates deer antler regeneration
- Park HJ, Lee DH, Park SG, Lee SC, Cho S, Kim HK, Kim JJ, Bae H, Park BC (2004) Proteome analysis of red deer antlers. Proteomics 4: 3642–3653. https://doi.org/10.1002/pmic.200401027
- Price J, Faucheux C, Allen S (2005a) Deer antlers as a model of mammalian regeneration. Curr Top Dev Biol 67:1–48. https://doi.org/10. 1016/S0070-2153(05)67001-9
- Price JS, Allen S, Faucheux C, Althnaian T, Mount JG (2005b) Deer antlers: a zoological curiosity or the key to understanding organ regeneration in mammals? J Anat 207:603–618. https://doi.org/10. 1111/j.1469-7580.2005.00478.x
- Rabinovich GA, Liu FT, Hirashima M, Anderson A (2007) An emerging role for galectins in tuning the immune response: lessons from experimental models of inflammatory disease, autoimmunity and cancer. Scand J Immunol 66:143–158. https://doi.org/10.1111/j.1365-3083.2007.01986.x
- RJ G (1983) Deer antlers. regeneration, function and evolution. Academic Press, New York
- Rolf HJ, Kierdorf U, Kierdorf H, Schulz J, Seymour N, Schliephake H, Napp J, Niebert S, Wölfel H, Wiese KG (2008) Localization and

- characterization of STRO-1 cells in the deer pedicle and regenerating antler. PLoS One 3:e2064. https://doi.org/10.1371/journal.pone.0002064
- Santelli G, Califano D, Chiappetta G, Vento MT, Bartoli PC, Zullo F, Trapasso F, Viglietto G, Fusco A (1999) Thymosin beta-10 gene overexpression is a general event in human carcinogenesis. Am J Pathol 155:799–804
- Seo MS, Park SB, Choi SW, Kim JJ, Kim HS, Kang KS (2014) Isolation and characterization of antler-derived multipotent stem cells. Cell Transplant 23:831–843. https://doi.org/10.3727/096368912X661391
- Sherbet GV (2009) Metastasis promoter S100A4 is a potentially valuable molecular target for cancer therapy. Cancer Lett 280:15–30. https:// doi.org/10.1016/j.canlet.2008.10.037
- Sribenja S, Li M, Wongkham S, Wongkham C, Yao Q, Chen C (2009) Advances in thymosin beta10 research: differential expression, molecular mechanisms, and clinical implications in cancer and other conditions. Cancer Investig 27:1016–1022. https://doi.org/10.3109/07357900902849640
- Stocum D (2006) Regenerative biology and medicine. Academic Press, New York
- Torti SV, Torti FM (2013) Iron and cancer: more ore to be mined. Nat Rev Cancer 13:342–355. https://doi.org/10.1038/nrc3495
- Wang D, Guo Q, Ba H, Li C (2016) Cloning and characterization of a Nanog pseudogene in sika deer (Cervus nippon). DNA and Cell Biology 35:576–584. https://doi.org/10.1089/dna.2016.3303
- Wang DT, Chu WH, Sun HM, Ba HX, Li CY (2017) Expression and functional analysis of tumor-related factor S100A4 in antler stem cells. J Histochem Cytochem 65:579–591. https://doi.org/10.1369/ 0022155417727263
- Yan KS, Gevaert O, Zheng GXY, Anchang B, Probert CS, Larkin KA, Davies PS, Cheng ZF, Kaddis JS, Han A, Roelf K, Calderon RI, Cynn E, Hu X, Mandleywala K, Wilhelmy J, Grimes SM, Corney DC, Boutet SC, Terry JM, Belgrader P, Ziraldo SB, Mikkelsen TS, Wang F, von Furstenberg RJ, Smith NR, Chandrakesan P, May R, Chrissy MAS, Jain R, Cartwright CA, Niland JC, Hong YK, Carrington J, Breault DT, Epstein J, Houchen CW, Lynch JP, Martin MG, Plevritis SK, Curtis C, Ji HP, Li L, Henning SJ, Wong MH, Kuo CJ (2017) Intestinal enteroendocrine lineage cells possess homeostatic and injury-inducible stem cell activity. Cell Stem Cell 21:78–90 e76. https://doi.org/10.1016/j.stem.2017.06.014
- Yu PJ, Lin W (2016) Single-cell transcriptome study as big data. Genom Proteom Bioinf 14:21–30. https://doi.org/10.1016/j.gpb.2016.01.005
- Zhang X, Ren D, Guo L, Wang L, Wu S, Lin C, Ye L, Zhu J, Li J, Song L, Lin H, He Z (2017) Thymosin beta 10 is a key regulator of tumorigenesis and metastasis and a novel serum marker in breast cancer. Breast Cancer Res 19:15. https://doi.org/10.1186/s13058-016-0785-2
- Zhang W, Chu W, Liu Q, Coates D, Shang Y, Li C (2018) Deer thymosin beta 10 functions as a novel factor for angiogenesis and chondrogenesis during antler growth and regeneration. Stem Cell Res Ther 9:166. https://doi.org/10.1186/s13287-018-0917-y
- Zheng GX et al (2017) Massively parallel digital transcriptional profiling of single cells. Nat Commun 8:14049. https://doi.org/10.1038/ncomms14049

